15 OCTOBER 1974

EXPERIMENT DEFINITION PHASE SHUTTLE LABORATORY

LDRL 10.6 EXPERIMENT

First Quarterly Report

NASA Contract NAS 5-20018

HUGHES
HUGHES AIRCRAFT COMPANY
SPACE AND COMMUNICATIONS GROUP

Hughes Ref. No. D0824 • SCG 40355R

15 OCTOBER 1974

EXPERIMENT DEFINITION PHASE
SHUTTLE LABORATORY

LDRL 10.6 EXPERIMENT

•

First Quarterly Report

NASA Contract NAS 5-20018

HUGHES
HUGHES AIRCRAFT COMPANY
SPACE AND COMMUNICATIONS GROUP

Hughes Ref. No. D0824 • SCG 40355R

CONTENTS

ERRATA TO

EXPERIMENT DEFINITION PHASE SHUTTLE LABORATORY

1) Page 1-2, Table 1-1:

   Doppler frequency, MHz should read
   -942 instead of 136

2) Page 3-3, last line:

   Replace ±136 by -942

3) Page 3-5, Figure 3-2(b); ordinate should read:

   DOPPLER FREQUENCY, MEGAHERTZ x10

4) Page 3-6, Replace page:

   New page 3-6 enclosed

1. INTRODUCTION AND SUMMARY

This first quarterly report for the Experiment Definition Phase of the Shuttle Laboratory LDRL-10.6 Experiment (Contract No. NAS 5-20018) covers the activities from 26 June to 26 September 1974.

The first month of the contract was devoted to the generation of the contract program plan.

The second month of the contract was devoted to establishing system requirements and defining preliminary system configurations. Work was also started in preliminary system parameter optimization. During the second month the PERT diagram for the study was also established.

The third month's main effort was the preliminary system optimization. During this month, by the initiation of the customer, it became apparent that the first experimental deployment of an LDRL-10.6 link will involve the shuttle in a low earth orbit to an elliptical orbit (preferably Moliniya orbit) satellite and the shuttle to a ground station. The elliptical orbit satellite terminal is under current development, and the ground terminals are more or less in existence. Under these conditions, priority has been given to the experiment definition to be carried by the shuttle. The shuttle terminal definition has therefore been the first task to consider.

From the various packages under study, a two gimbal system, termed package B, was selected. This configuration was selected on the belief that it will lead more directly to the ultimate deployment of this terminal on a dedicated low earth orbit satellite. It was felt that in the long run this approach will lead to substantial savings because the shuttle terminal may be considered to be the engineering model of the actual mission terminal. Cost savings will be implemented using the facilities of the shuttle. Electronics will be rack-mounted inside the Space Lab Module of the shuttle and shorter shuttle lifetime specifications will result in cost savings.

The key transmit and receive parameters have been subjected to an optimization program to pick the best values to provide required performance at a minimum weight. The parameters listed in Table 1-1 have been calculated from this weight optimization study.

TABLE 1-1. CHARACTERISTICS OF OPTIMAL SPACEBORNE TERMINALS

Characteristic	Shuttle Terminal Package B	Molniya Terminal Package A
Aperture diameter, cm	22.4	22.6
Laser output power, W	0.60	NA
Point ahead angle, maximum μrad	50	
Doppler frequency, MHz	–	136
Prime power required, W	165	152
Weight, lb	116	115

2. PROGRAM PLAN

The program plan was included as an appendix to the first monthly report while the associated, finalized PERT was included in the second monthly report. These items will not be repeated here.

3. SYSTEM REQUIREMENT DEFINITION

The system requirements include mission requirements and parameter requirements derived from the particular mission scenario.

3.1 MISSION REQUIREMENTS

3.1.1 Transmission Rate

Transmission rate to be no less than 400 Mbps.

3.1.2 Bit Error Rate

The bit error probability is defined by no less than 10^{-6}.

3.1.3 Link Establishment and Maintenance Requirements

An acquisition and tracking study is currently being performed. The output of this study, in addition to providing an acquisition and tracking scheme, will determine bounds and parametric relationships among probability of acquisition, probability of false acquisition, mean time to acquisition, and probability of loosing track.

3.1.4 Lifetime

The lifetime of the shuttle-borne instrumentation is defined with customer consent, to be a maximum of 30 days. In addition, equipment and structure attachments must be certified to withstand the crash safety shock without breaking loose and creating a hazard to personnel or preventing egress from a crashed shuttle vehicle.

This environmental requirement may be satisfied by the static structural stress analysis. Testing should only be performed on those items not covered in the stress analysis. The payload design goal for crash safety shock has a sawtooth time response with a 40 ±6 g peak value over an 11 ms duration.

3.1.5 Vibration Specifications

Flight

The Space Shuttle vehicle will be subjected to fluctuating pressure loading on its exterior surfaces by engine exhaust, generated acoustic noise, and air flow generated aerodynamic noise during powered ascent through the atmosphere. These fluctuating pressure loads are the principal sources of structural vibration.

The estimated random vibration for the cabin and midfuselage payload interface due to the fluctuating pressure loads is shown in Figure 3-1. These vibration levels exist for approximately 29 seconds per mission. The reentry vibration environment is negligible. Actual vibration input to payloads will depend on the transmission characteristics of the midfuselage, the payload support structure, and interactions with each payload's weight, stiffness, and cg.

Transient Vibration. Events such as gust loading, engine ignition and cutoff, and separation and docking will induce low frequency transient responses in the Space Shuttle vehicle. The response for each event for various locations will be calculated. However, for the interim the overall effect of these transient events is accounted for by a swept sinusoidal vibration environment imposed in the frequency range from 5 to 35 Hz at an acceleration amplitude of ±0.25 g peak.

Ground

The ground vibration spectrum that the payloads are expected to experience is a minimum of four sweeps at 1/2 octave per minute at the following levels (sinusoidal motion):

2 to 5 Hz at 1.0 inch double amplitude
5 to 26 Hz at 1.3 g peak
26 to 500 Hz at 0.36 inch double amplitude
500 to 1000 Hz at 5 g peak

3.2 PARAMETER REQUIREMENTS

The parameters for the two primary links that affect the design of the space package include:

1) Range, Km

2) Doppler Frequency, MHz

3) Point Ahead Angle, μrad

4) Azimuth angle in the local tangent plane from true north, degrees

5) Azimuth angle from local vertical, degrees

6) Elevation angle from local vertical, degrees

7) Elevation angle rate, deg/min

8) Total angular rate – vector sum of azimuth and elevation rate, deg/min

Parameter requirements are based on orbital link deployments. The link deployments considered here are the shuttle to ground and the shuttle to elliptical orbit of minimal apsidal rotation (Molniya) and with a 12 hour period.

At present the orbits of shuttle and Molniya orbit satellite have not been established. The prevailing thought in defining these orbits is to establish parameter extremes. Experiment designs will then encompass these extremes.

3.2.1 Shuttle to Ground Link Parameter Requirements

The shuttle is considered to be on circular equatorial orbit at an altitude of 185 km (100 n.mi.) which passes directly over the ground station. At zero time the satellite is directly over the ground station.

The time histories of the parameters have been plotted for zenith angles up to 60° (30° above the horizon). Azimuth angle and angle rate are not plotted as they do not change. Parameter time histories are shown in Figure 3-2. It is seen that a maximum of the point ahead angle is about 50 μrad.

3.2.2 Shuttle to Molniya Parameter Requirements

The Molniya is a minimal apsidal rotation orbit inclined at 63.43° with an apogee of 39,438 km and a perigee of 926 km. For maximum doppler frequency consideration, the shuttle orbit is taken to be a circular coplanar orbit at an altitude of 185 km. As a matter of calculating convenience both orbits have been reduced to equatorial (zero inclination). Figure 3-3 gives the time histories of the parameters under study. It is seen that doppler frequency has a maximum of ±136 MHz.

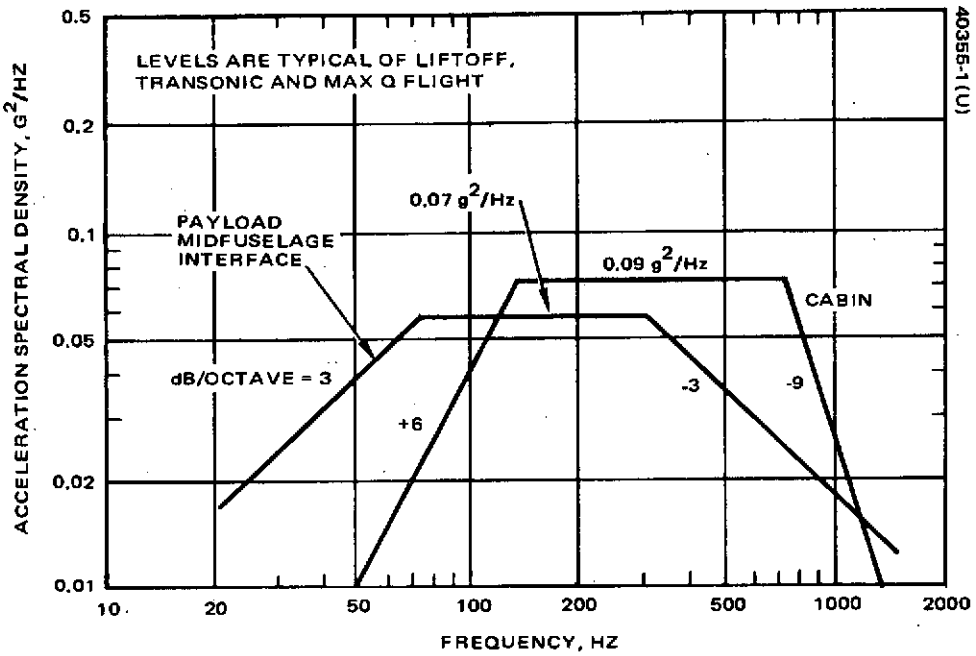

FIGURE 3-1. RANDOM VIBRATION AT PAYLOAD MIDFUSELAGE INTERFACE AND IN CABIN

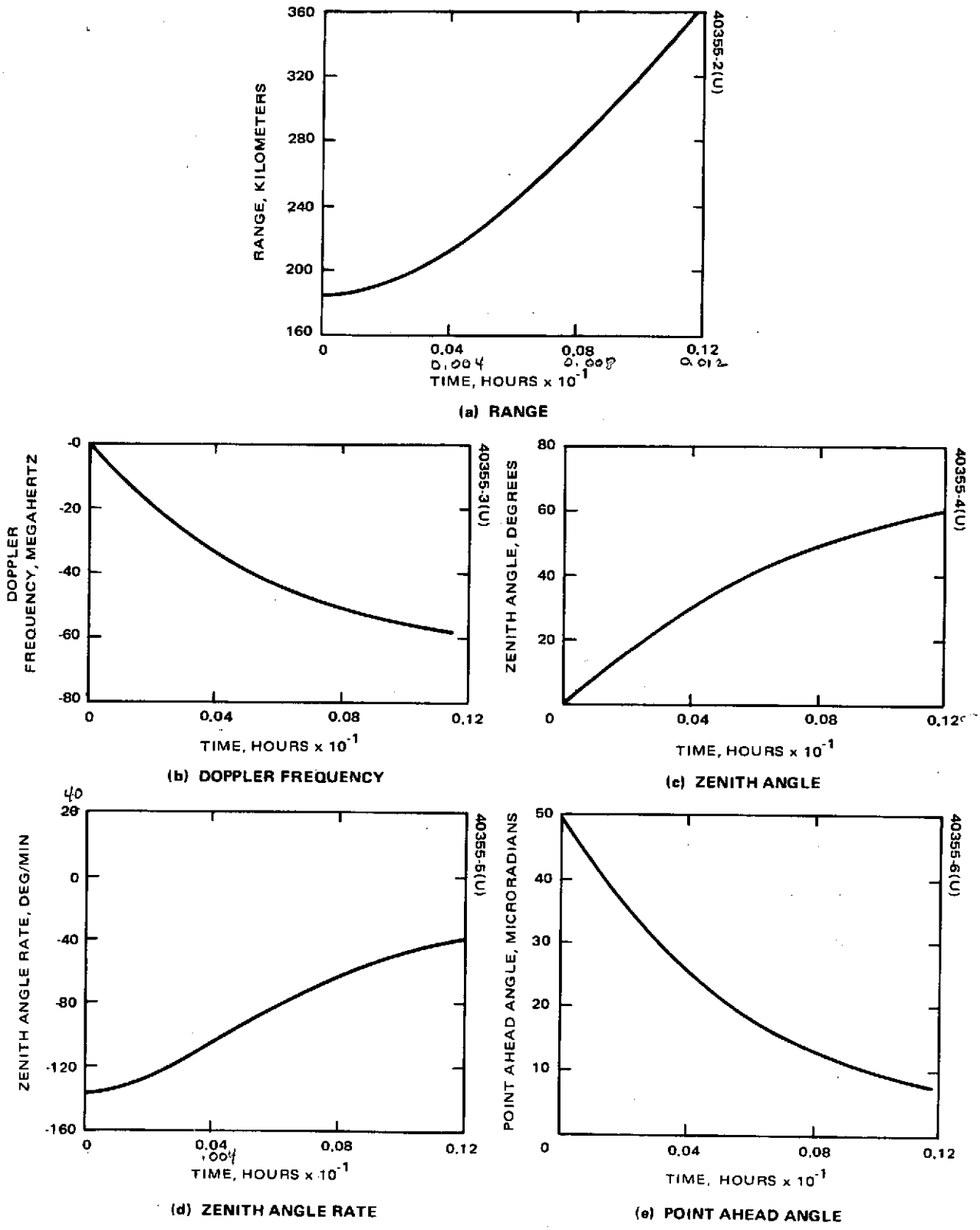

FIGURE 3-2. SHUTTLE TO GROUND LINK

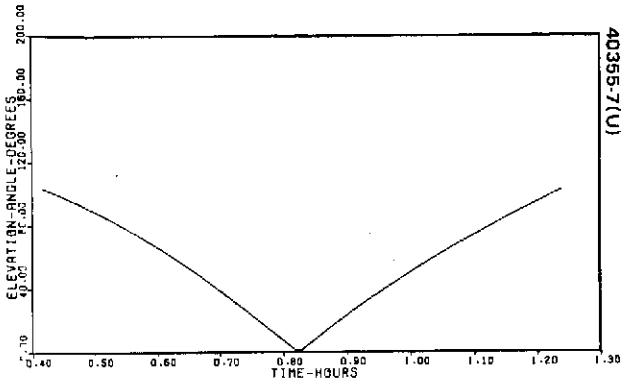

a) ELEVATION ANGLE

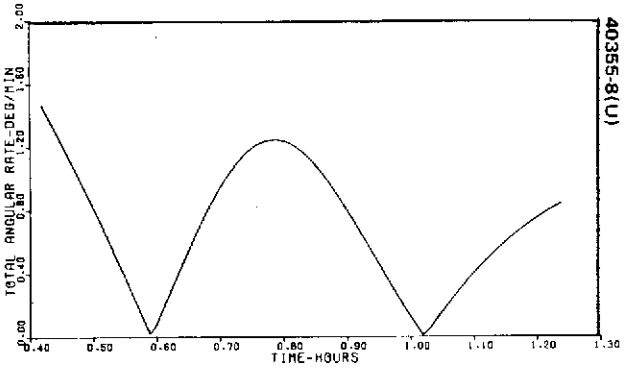

b) ANGULAR RATE

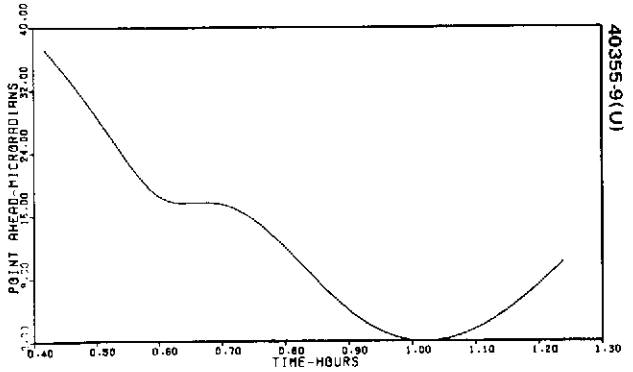

c) POINT AHEAD ANGLE

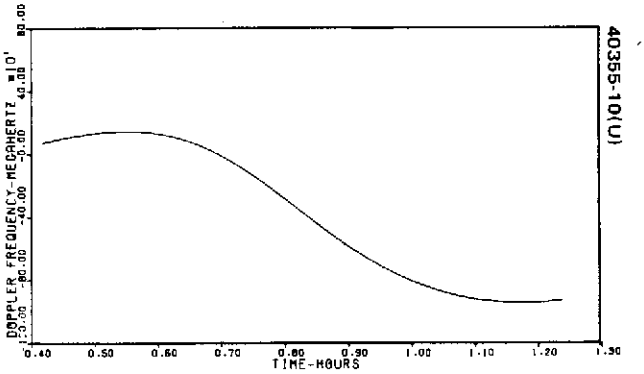

d) DOPPLER FREQUENCY

FIGURE 3-3. SHUTTLE TO MOLNIYA ORBIT

4. PRELIMINARY SYSTEM CONFIGURATION AND DESIGN

4.1 DEFINITION OF PACKAGES

The shuttle terminal configurations considered in the experiment definition study are defined as packages and are included in Table 4-1. For completion, the high altitude transceiver terminal has been included as Package A.

Package D has been rejected from further consideration (see 4.3.1). Package C, considered to be either the progenitor of Package B or the modified Package A, mounted on a course positioned platform. This last solution was examined briefly, but was rejected because it offers no potential for further development into an operational system. Thus the progenitor of Package B was selected as the most promising long term solution. In order to simplify nomenclature, this package is named Package B. It is essentially the brassboard model of the deployed Low Earth Orbit satellite (LEOS) terminal.

TABLE 4-1. PACKAGE DEFINITION

Subsystem	Packages				Remarks
	A Synchronous or Elliptic Orbit Satellite	B Deployed Lower Orbit Satellite	C Shuttle	D Shuttle	
Receiver	X				
Transmitter		X	X	X	
Opto-mechanical					
Mod 1	X				Pointing coverage $25^{o} \times 25^{o}$
Mod 2		X			Pointing coverage 2πsr
Mod 2a or 1a			X		Progenitor of B or modified A for coverage of 2πsr
Mod 3				X	Coudè configuration
Cooler					
Radiation	X				
Telemetry and Command	X	X	X	X	Common to all packages

4.2 OPTO-MECHANICAL CONSIDERATIONS

4.2.1 Gimbal Selection

The opto-mechanical subsystem has the requirement to acquire and maintain the line of sight to the Molniya, or the ground, receiver from a low altitude shuttle spacecraft. The mechanical design requirements on the low altitude transmitter present a difficult task, because hemispherical gimbal coverage is required to accommodate the orbital motion of the LEO spacecraft. Hemispherical coverage requires, in general, three axes or gimbals to prevent "gimbal lock" at all view angles. A two-axis system can, however, basically meet the pointing requirements in a less expensive way. Thus, for the Package B, a two-axis gimbal configuration using an X-Y pattern is being considered.

This choice avoids the complexity of the three-axis system but has the disadvantage of blind angular cones at the horizon. Such blind areas can be handled in the following three ways:

1) Pitch the LEO spacecraft twice a day during the period that the satellite is behind the earth (i.e., the spacecraft is the third axis) such that the active tracking will not require the blind angular zones.

2) Limit the communications during the obscured period.

3) Limit the communications during mid-orbit (overhead pointing) by using an elevation/azimuth gimbal combination.

Either of the two-axis combinations (2 and 3 above) has limited viewing on only two of the 16 daily orbits.

The hemispherical coverage in the baseline design includes an inner gimbal (tilt axis) that rotates a folding mirror ±75°. This avoids the gimbal lock region. The obscured areas, therefore, are ±15°. The outer gimbal (roll axis) has limited rotation also, but can slightly exceed ±90° to ensure the horizon look angle. With limited rotation in both axes, simple flex electrical cables can be used instead of slip rings.

Pointing control for acquisition and tracking is provided by a two stage mechanism. Coarse pointing consists of the flat pointing mirror and gimbal assembly. The flat mirror is mounted in a yoke on a rotatable pedestal. Rotation of the entire pedestal/mirror assembly provides the azimuth or roll sweep of the mirror while elevation positioning is obtained by declination or tilt of the mirror about its pivot axis in the yoke. Positioning is independent in each axis and is accomplished by a stepper motor drive. The positioning drive for each axis consists of spur gear reduction from the motor shaft to a final output stage which is a single thread worm gear engaging a short, matching worm wheel. The use of such a final stage permits utilization of a unidirectional spring load at the axis pivot to remove backlash. The overall gear reduction for the tilt axis needs to be twice that of the roll axis to achieve the same effective beam displacement per motor step due to the optical doubling effect inherent in the tilt axis.

Fine angular positioning is achieved by means of an image motion compensator (IMC) in each axis. These compensators consist of small mirrors within the optical path mounted on the output coil of a piezoelectric driver. The image motion compensators provide raster search as well as conical scan capability.

The transmitter opto-mechanical subsystem is composed of the following elements:

1) Structure
2) Gimbal elements including bearings, gear reductions, gimbal angle encoders, resolvers, and motors
3) Optical subsystem
4) Mounting provisions for optics system and IMCs
5) Servo electronics and power conditioner
6) Interconnect cabling

4.2.2 Weight Function Relationships

The selection of major parameter values will be made on the basis of the lightest weight system. In order to perform an optimization calculation, it is necessary to model the components in the package relative to weight. This modeling has been done on past contracts for most of the components; however, it was updated for this study. The following is that modeling analysis.

Outline drawings, Figures 4-1 through 4-4, were prepared to identify the principal areas of weight growth for large aperture systems of the transmitter. Two possible gimbal bearing configurations for a 10 inch f/2 system are shown in Figures 4-2 and 4-3. The outer gimbal bearing arrangement shown in Figure 4-2 is the same as the configuration for the 5 inch aperture system; however, if after a detailed analysis of bearing loads it is indicated that greater capacity is required, one possible configuration is that shown in Figure 4-3.

Estimated weights of major subsystem categories for the receiver and transmitter were curve fit, and the resultant computer generated curves are presented in Figure 4-5. The following conclusions may be drawn from these data.

Structure Versus Primary Aperture

In both cases, structure weight increases are the direct result of primary mirror diameter changes. Package B, however, is less sensitive in the structure category with the larger impact in the gimbal, motors, and steering mirror category.

Optical Telescope Versus Primary Aperture

The relationship of weight increase to aperture diameter is basically a cubic for both Package A and B. The higher weight of Package B is due to the additional folding mirror required for the transmitter.

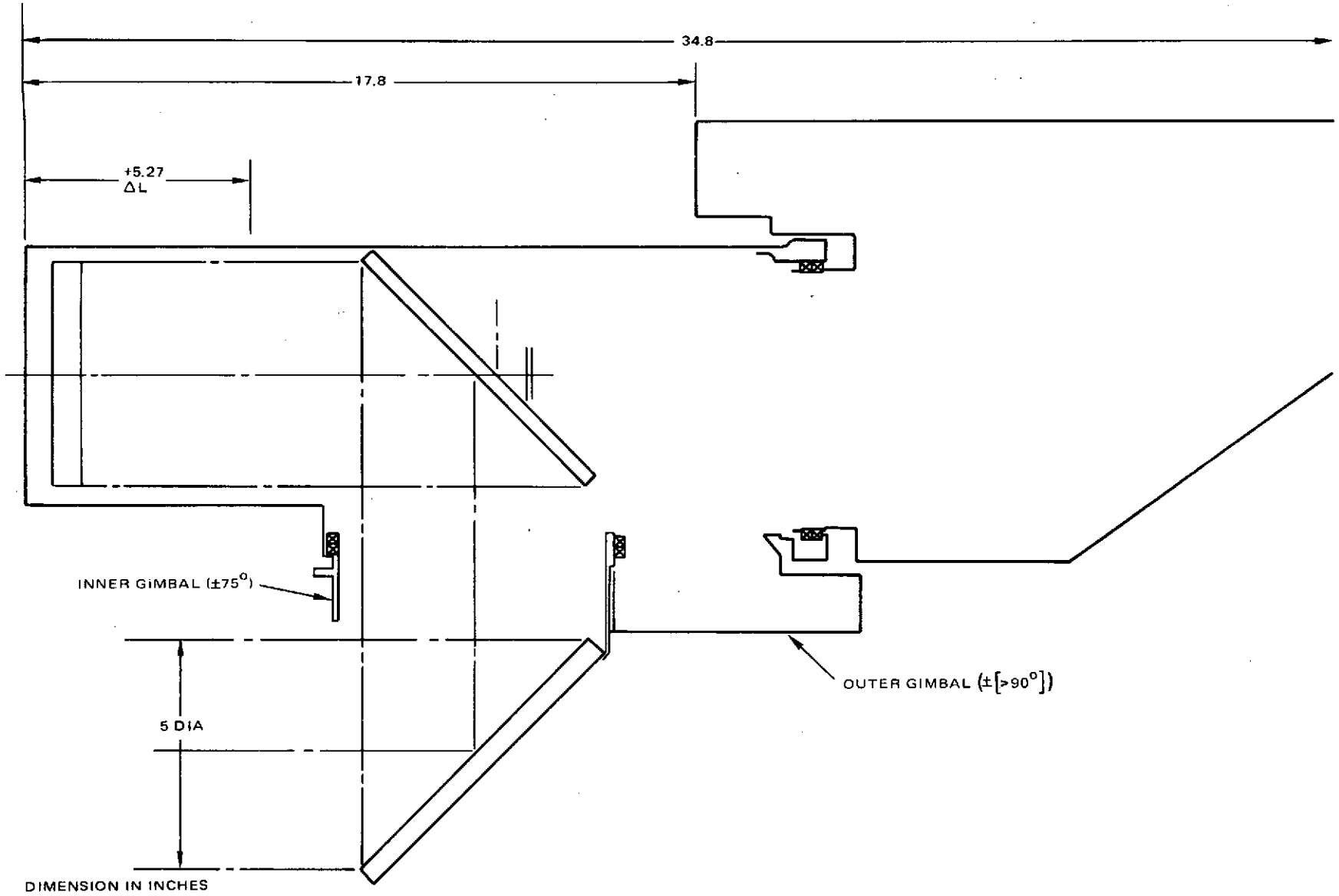

FIGURE 4-1. PACKAGE B – 5 INCH OPTICS F/2 SYSTEM

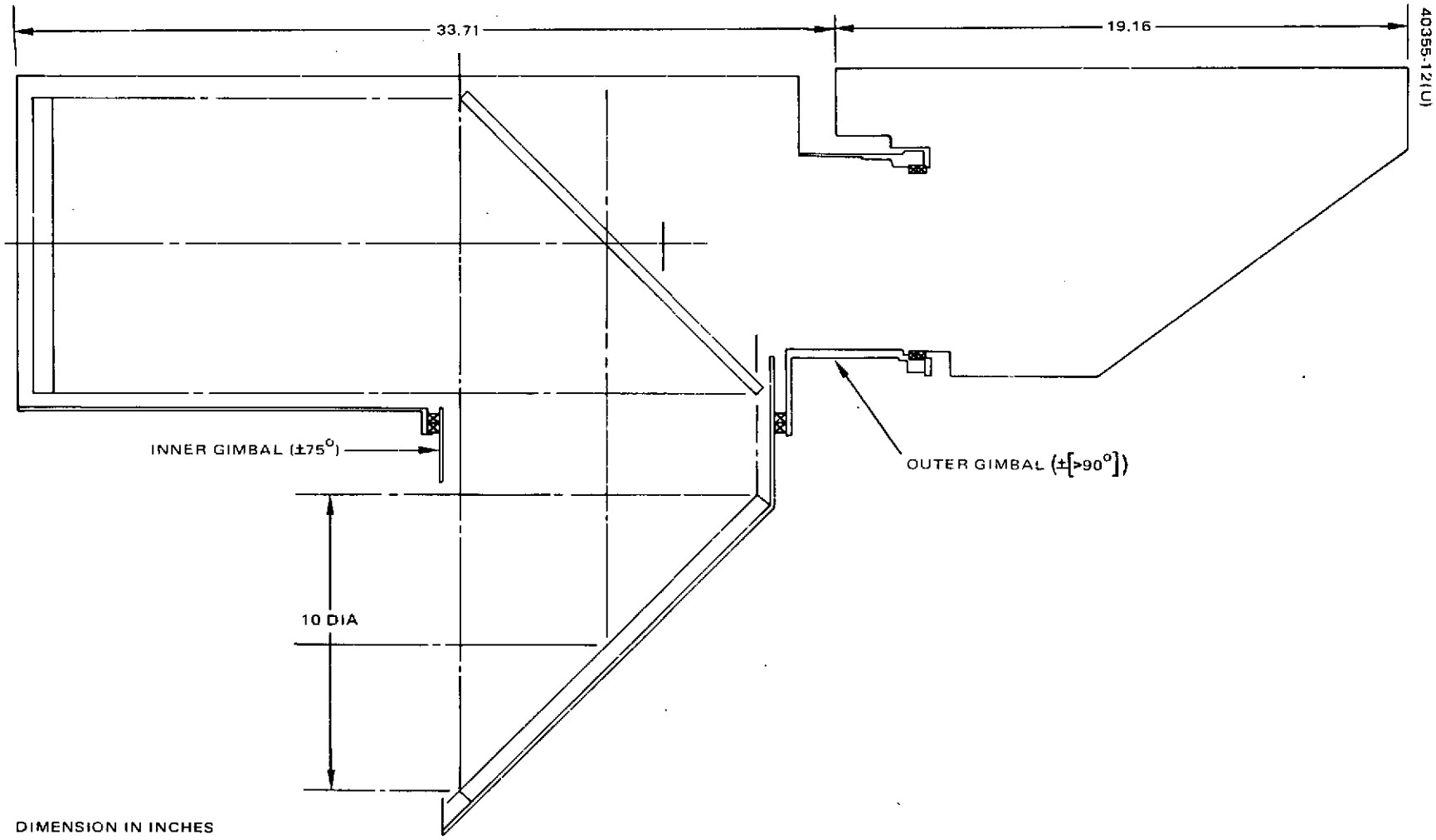

FIGURE 4-2. PACKAGE B – 10 INCH OPTICS F/2 SYSTEM

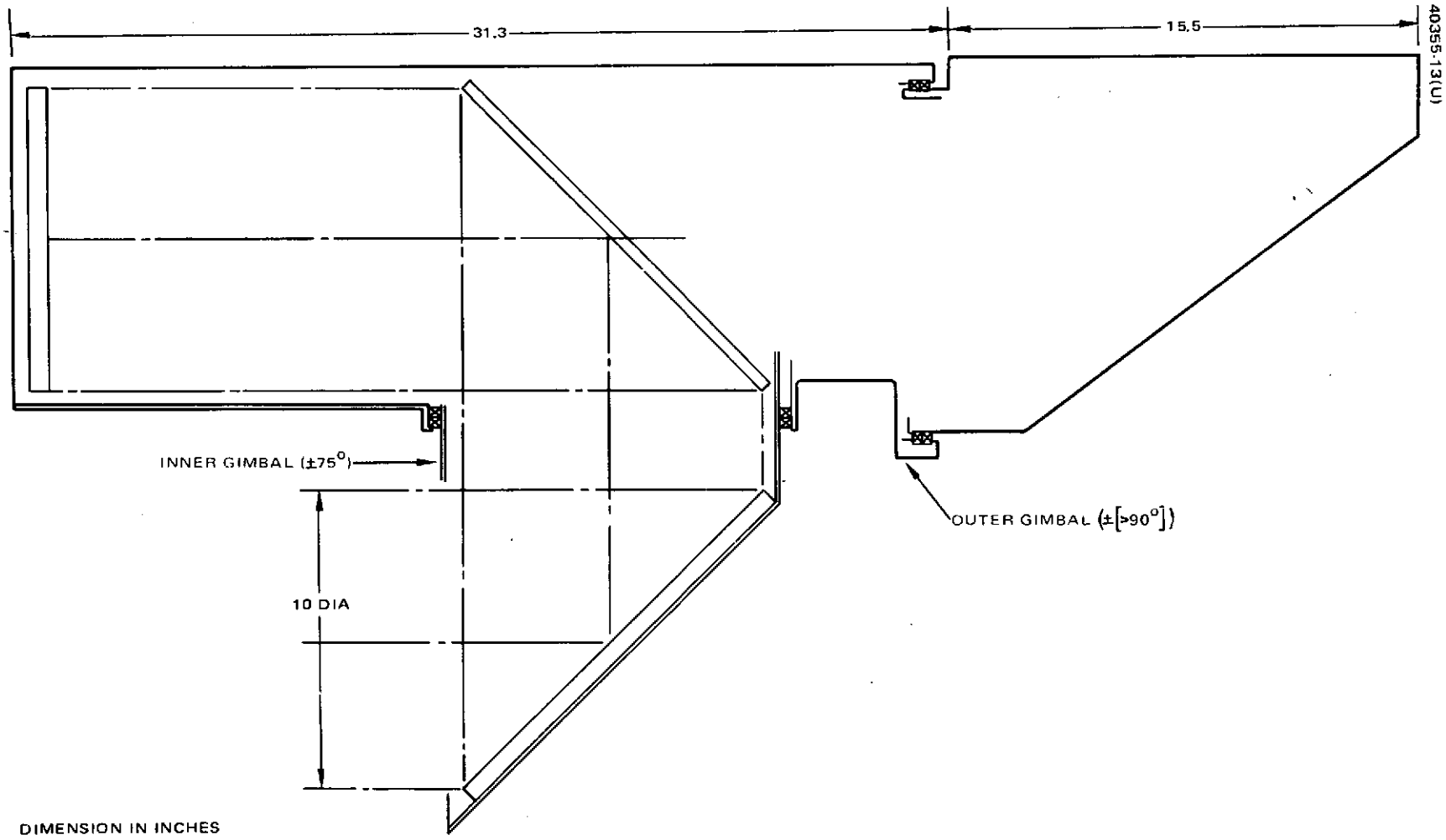

FIGURE 4-3. PACKAGE B – 10 INCH OPTICS F/2 SYSTEM, LARGER OUTER GIMBAL BEARING

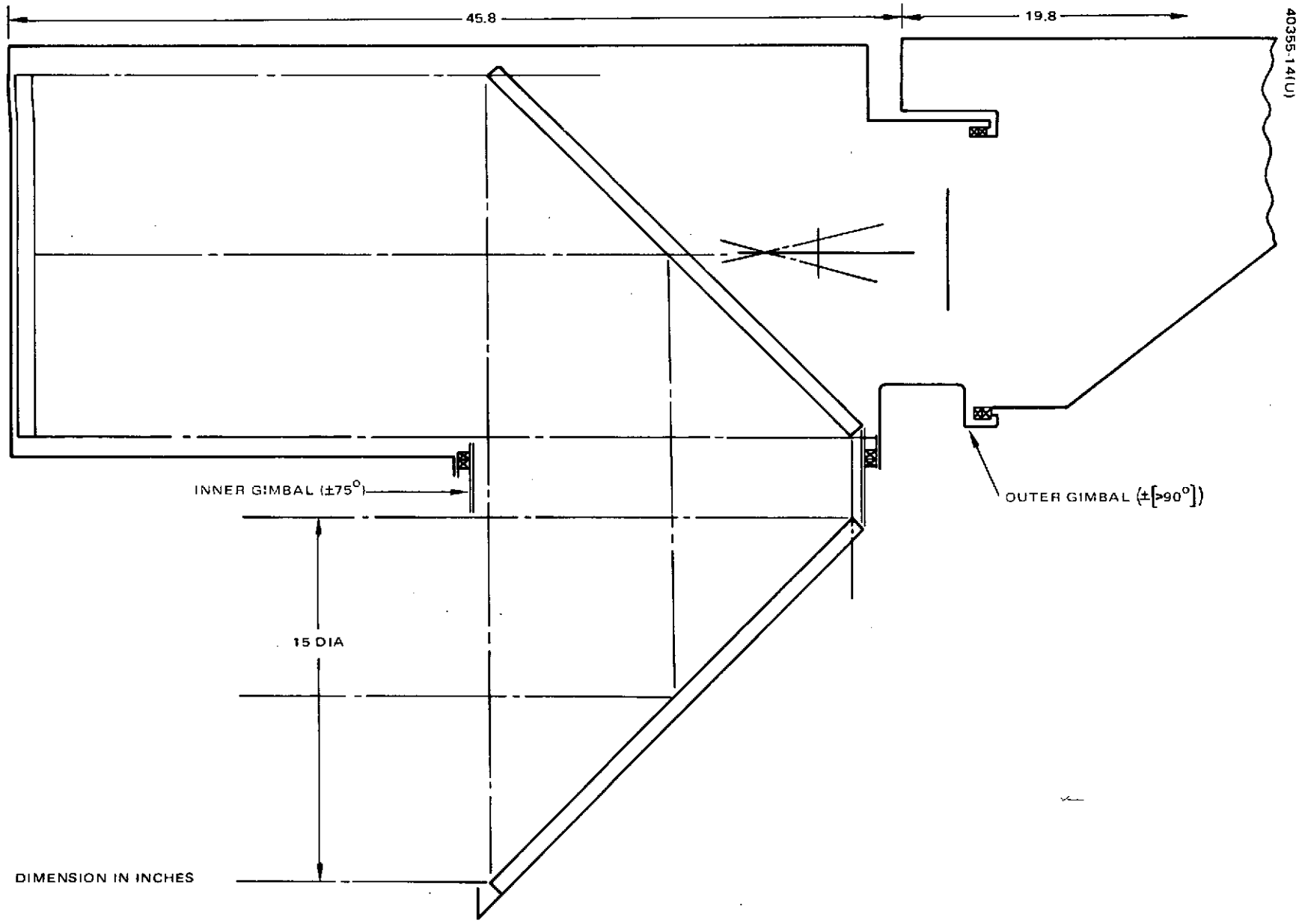

FIGURE 4-4. PACKAGE B – 15 INCH OPTICS F/2 SYSTEM

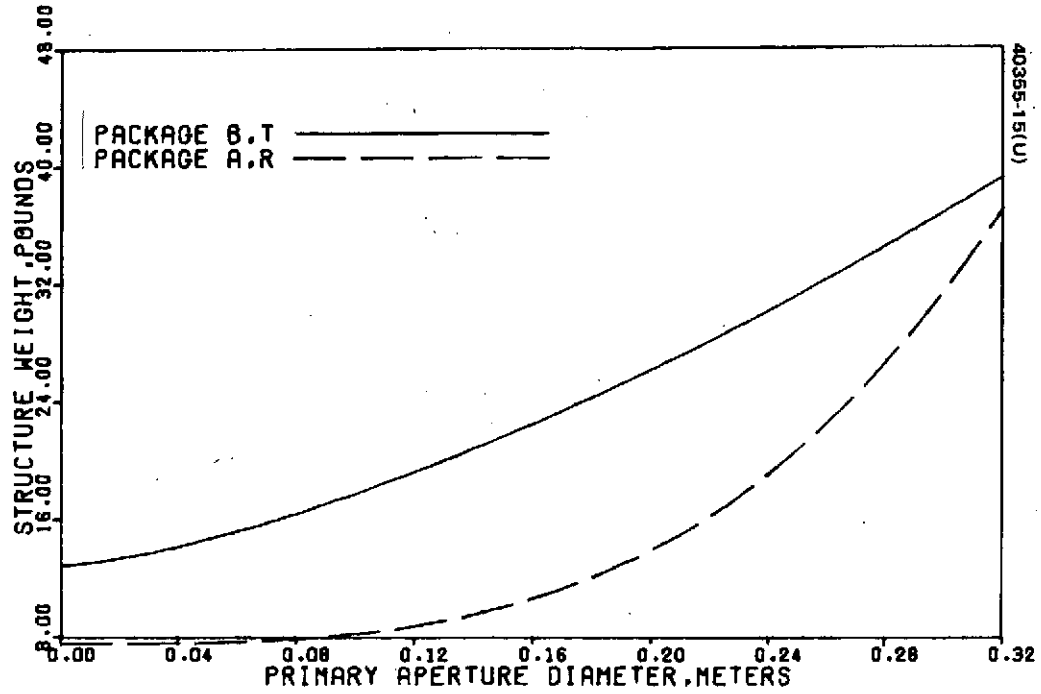

a) STRUCTURE

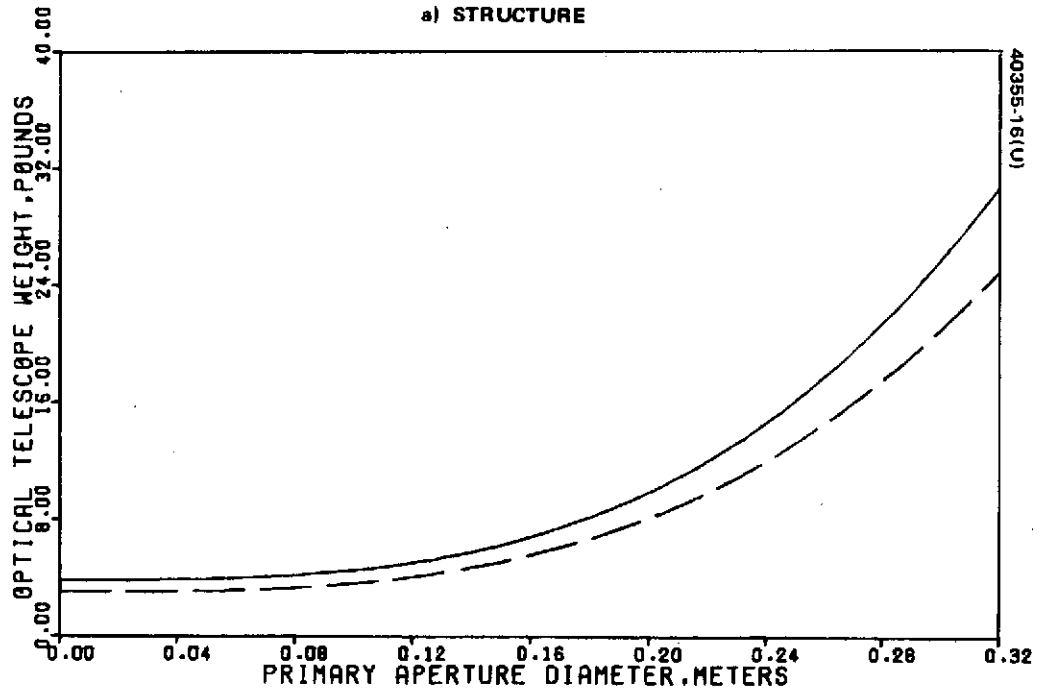

b) TELESCOPE

FIGURE 4-5. ESTIMATED SUBSYSTEM WEIGHT

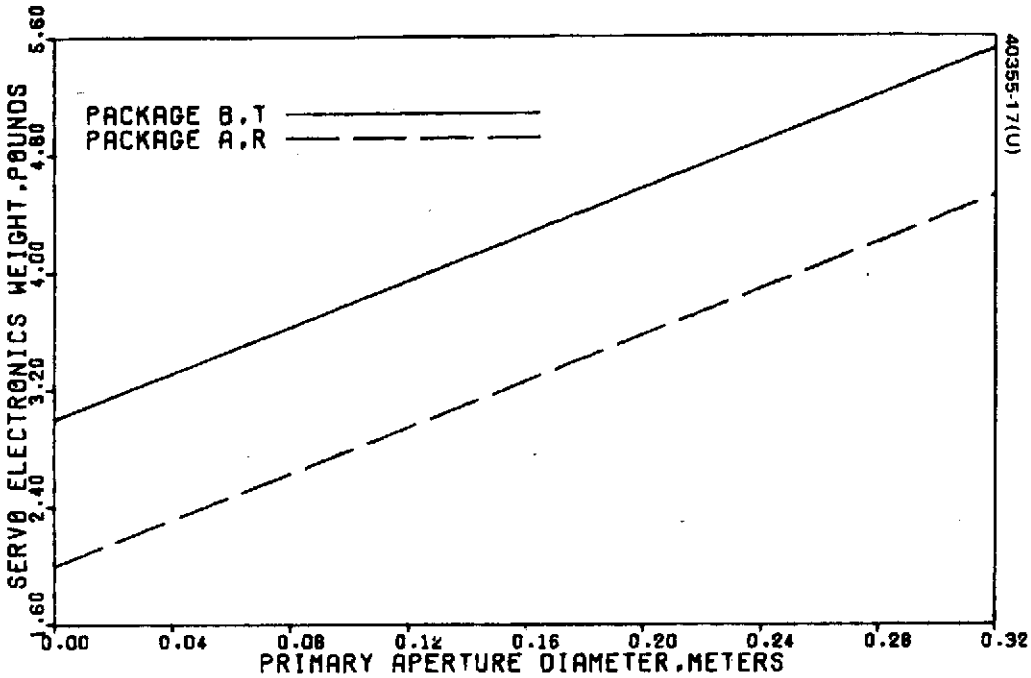

c) SERVO ELECTRONICS

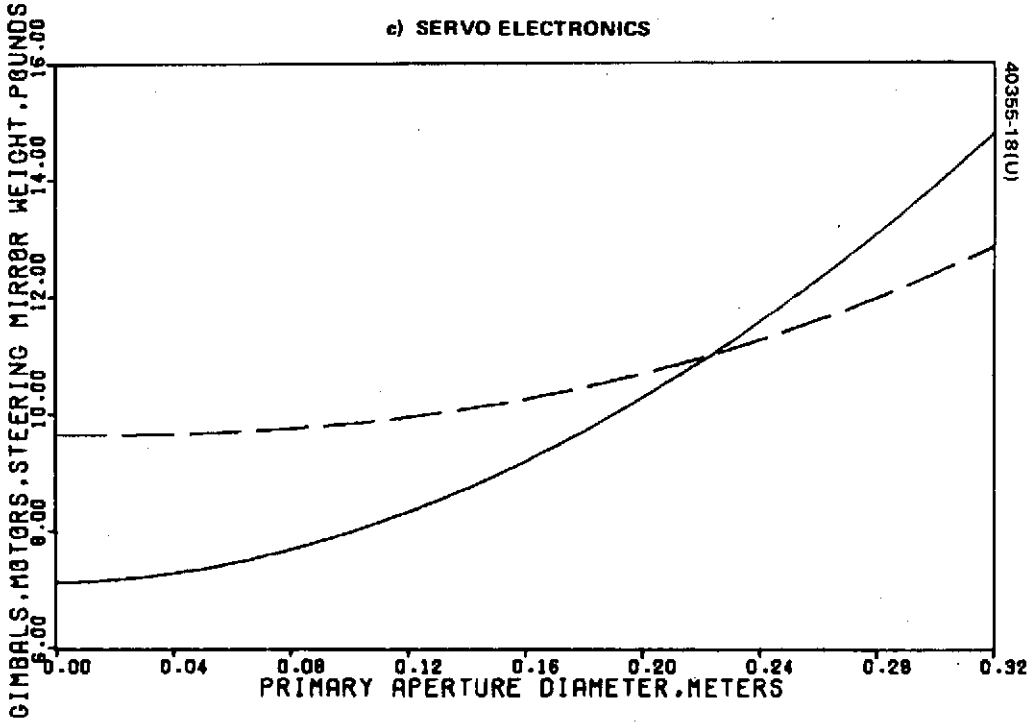

d) GIMBALS AND DRIVES

FIGURE 4-5 (CONTINUED). ESTIMATED SUBSYSTEM WEIGHT

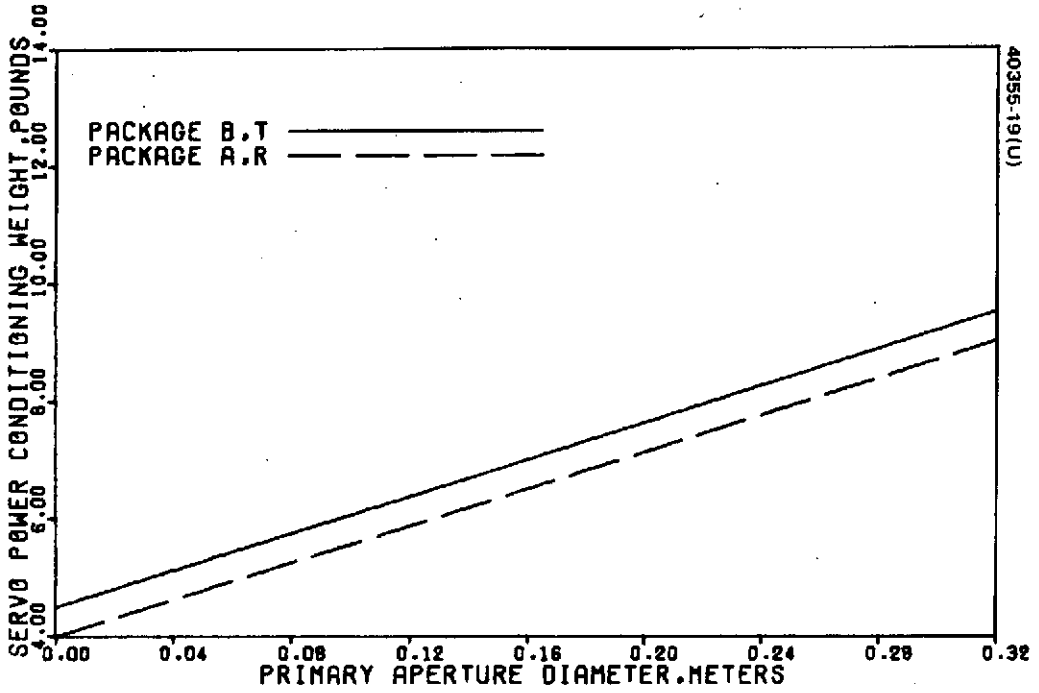

e) SERVO POWER CONDITIONING

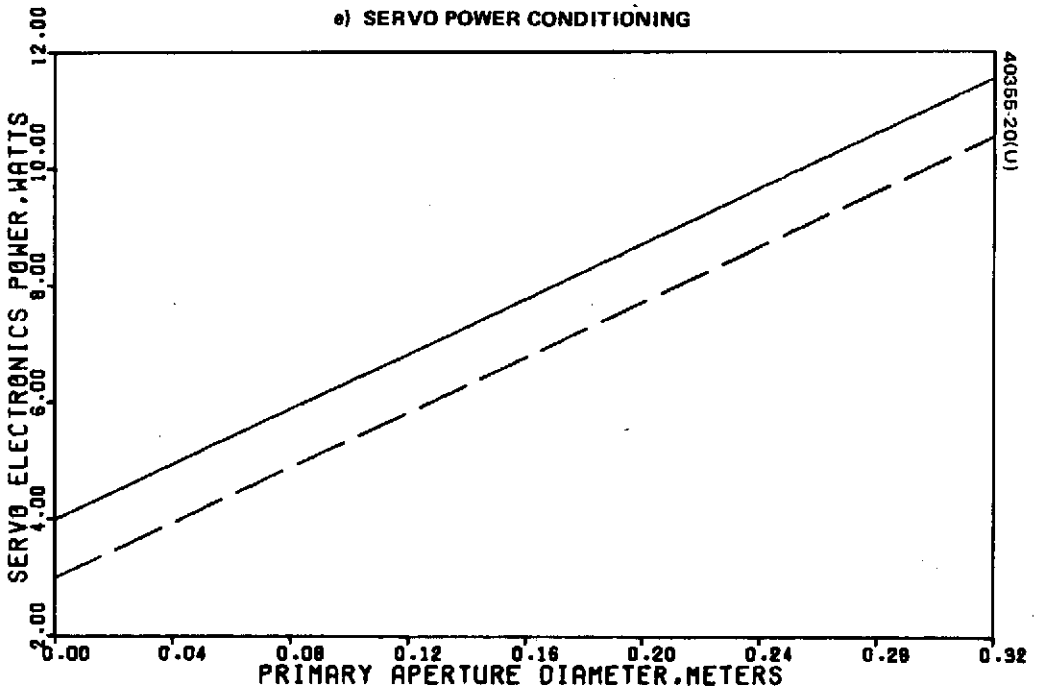

f) SERVO ELECTRONICS POWER

FIGURE 4-5 (CONTINUED). ESTIMATED SUBSYSTEM WEIGHT

Servo Electronics Weight and Power

The greater weight and power required for Package B over that of Package A is specifically a result of the added requirement to drive and process resolvers and encoders for both axes. The wide gimbal angle requirement of Package B along with the condition of a fixed error sensor relative to the gimbaled mirrors means the servo system must compute coordinate transformations.

Gimbals, Motors, and Steering Mirror

Package A weight is primarily affected by mirror and yoke type, whereas Package B sizing for bearings, ring gear, and steering mirror is directly related to the optical clear aperture, which in this case goes through the inner gimbal bearing bore. For Package B, two bearing configurations are possible. The optimized bearing size, however, will depend upon a detailed analysis of bearing loads.

Servo Power Conditioner Weight

This reflects the added requirements of the servo electronics. The higher weight of Package B servo power conditioner is a result of converter and voltage regulation for the resolvers and encoders not used in Package A.

Image Motion Compensation Subsystem

Estimates for IMC systems were included in the weight data; however, a single size device now exists and, therefore, it may be necessary to limit the acquisition field or design a new IMC device.

4.3 OPTICAL CONSIDERATIONS

4.3.1 Preliminary Study of System Configurations

A number of optical design solutions have been examined with regard to their applicability to the transmitter subsystem. The conclusions of this study are as follows.

Cassegrain Telescope With Coude Focal Positions

This type of telescope design generally has an alti-azimuth mount, and the viewing axis is stablized along the polar axis. For space applications, this design approach does not offer advantages over a Gregorian system (see next subsection), although the basic telescope design is compact. The compactness of the Cassegrain design comes about because it does not form a real primary image, but this can be a disadvantage when the system is required to be well baffled.

In order to maximize the output power of the laser transmitter, it is important to minimize the central obscuration of the telescope. In the case of the Cassegrain system, this implies that the focal length of the secondary mirror must be minimized with respect to that of the primary, and that a fast relay system will be needed to relocate the exit pupil to a convenient position so as to accommodate the image motion compensators. The addition of this relay system renders the Cassegrain telescope approach less attractive as compared with a simpler Gregorian design.

Gregorian Telescope With Cofocal Paraboloids

The Gregorian configuration has been studied in detail, and this type of telescope appears to offer the best design solution for laser transmitter. The output from the telescope is reflected out of the Gregorian system using a large folding mirror located with its center close to the focus of the primary mirror. This folding mirror has a small cutout in the center so as to permit light from the secondary mirror to reach the primary. This design approach minimizes the central obscuration of the output beam. The Gregorian configuration also permits the exit pupil to be positioned externally without the need for a separate relay system. Subsection 4.3.2 presents an example of a laser transmitter and beacon receiver system using the Gregorian telescope.

In designing an efficient Gregorian laser optical system, it is important to take into account the following:

1) The dependence of central obscurations on the f number of the primary mirror

2) The telescope FOV during acquisition

3) Methods for maximizing the output power in the presence of a given central obscuration

The above topics will be discussed in 4.3.3.

4.3.2 Two-Axis Laser Transmitter and Beacon Receiver Using Gregorian Afocal Telescope

The optical system shown in Figure 4-6 consists of a pointing mirror in front of a Gregorian afocal telescope subassembly. The afocal telescope consists of two cofocal paraboloids. A large folding mirror reflects the laser beam out of the system and directs the incoming beacon beam toward the primary mirror. A pair of image motion compensators are placed very close to the exit pupil of the telescope. This exit pupil is also the aperture stop of the system. It is relayed out of the telescope by a small folding mirror located in front of the secondary. Two folding mirrors direct the transmitted and received energy through the center of the outer gimbal. Behind the outer gimbal is a beam splitter. This beam splitter reflects the 0.9 μm beacon and transmits the 10.6 μm laser beams.

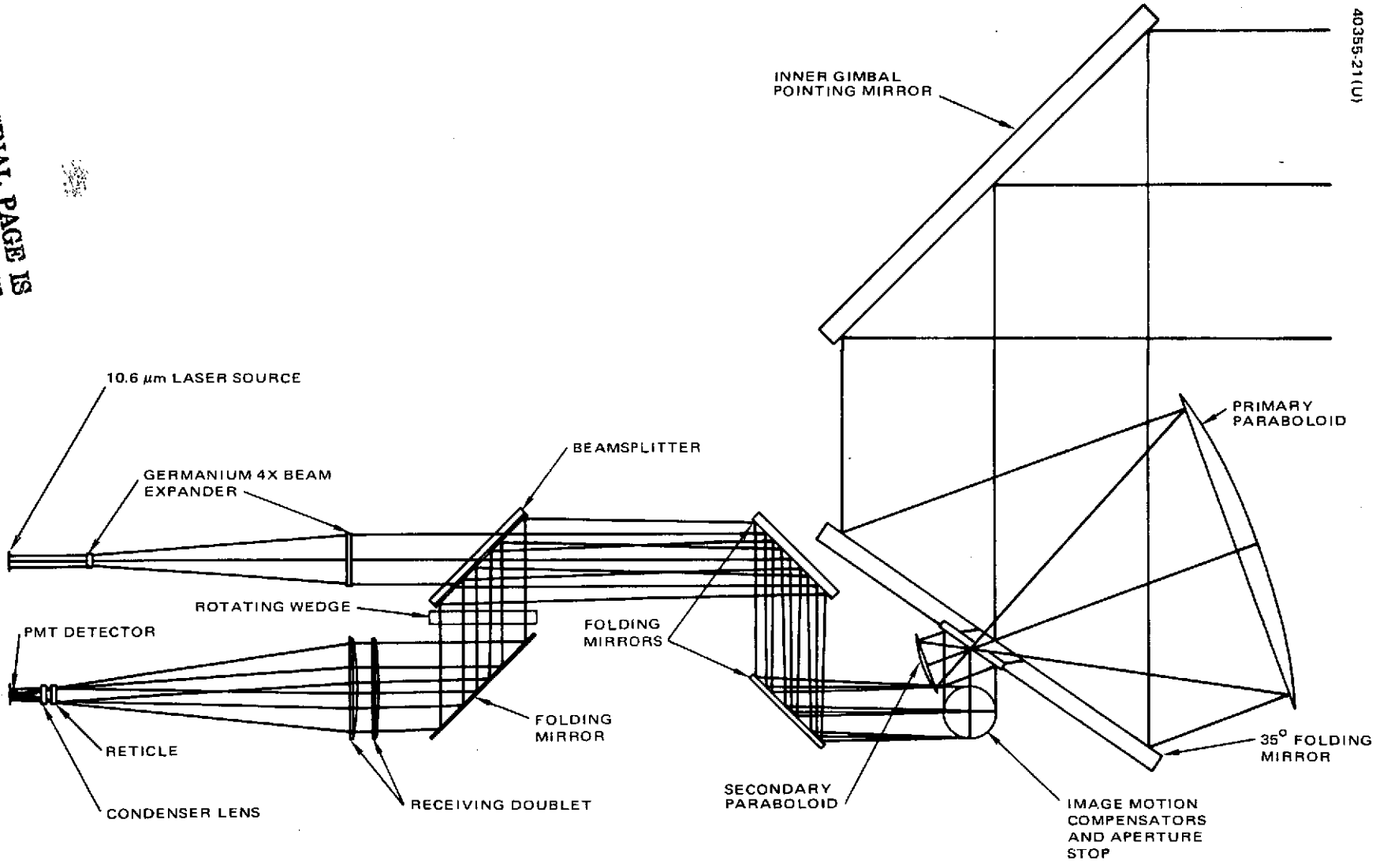

FIGURE 4-6. LASER TRANSMITTER AND BEACON RECEIVER OPTICAL SCHEMATIC

The transmitted laser beam will be suitably expanded (see 4.3.3) to match the input of the afocal telescope. Some details related to the expansion ratio of the laser beam expander, the central obscuration and the f number of the telescope will be considered in the following subsection.

4.3.3 Optical Design Considerations

The Gaussian beam profile of a CO_2 laser has its highest energy concentration in the center of the beam. This central portion of the beam would be lost in the presence of central obscuration. Figure 4-7 shows the percent energy obscured for uniform and Gaussian beams using a 12 cm aperture, the Gaussian profile being truncated at the $1/e^2$ point.

The central obscuration of the Gregorian telescope is essentially determined by the inside apertures in the folding mirrors. The sizes of these apertures are in turn dependent on the telescope acquisition FOV, θ. This is because these inside apertures must be sufficiently large so as not to obscure any part of the image field of the beacon beam during acquisition. The size of the image field, η, is given by

$$\eta = \theta \cdot f$$

where f is the focal length of the primary mirror. For the proposed laser transmitter system, θ = 17.45 mr (i.e., 1°). Thus, for a given θ and primary mirror diameter, D, the central obscuration can be minimized only if f is minimized. This implies that the f-number (= f/D) of the primary must be small if the power loss resulting from central obscuration is to be minimized.

Based on practical experience, the f-number of the primary should not fall much below f/1.5, lest the misalignment tolerances become extremely small. Here the advantage of having a very fast primary could easily be cancelled by the performance degradation resulting from residual misalignments. It is therefore recommended here that mirrors faster than about f/1.5 should not be considered as candidates for the laser transmitter. The effects of the resulting larger central obscuration upon the output power will have to be reduced by techniques other than the one using very fast mirrors.

There are at least two methods for reconstituting the Gaussian beam profile so as to minimize the output losses resulting from the central obscuration. These methods are outlined below:

Method One – This method requires the Gaussian beam from the CO_2 laser to be suitably expanded so as to overfill the aperture stop of the telescope (see Figure 4-6). By broadening the beam profile, the high energy central region will now spread more, and consequently a given central obscuration will cut off a smaller portion of the laser energy. The increase in the output power is achieved by truncating the low power $1/e^2$ regions of the beam profile and passing more of the high power regions.

Method Two — This method is based on the axicon, an energy redistribution device shown in Figure 4-8. Such a device can increase the far field peak irradiance by a factor of 2 when the diameter obscuration ratio is 0.25. Figure 4-9 compares antenna gains as a function of obscuration ratio for an optical telescope illuminated with a uniform irradiance beam, a Gaussian beam, and a Gaussian distribution modified by an axicon such as shown in Figure 4-8. The alignment tolerances for this device tend to be quite critical. The increased gain anticipated from its use must be weighed against possible degradation produced by its misalignment in the system and/or any wavefront deformation due to residual manufacturing errors.

Both methods will be examined in detail, and one of these solutions is expected to be incorporated into the final design.

4.3.4 Data Related to CO_2 Laser Transmitter and Receiver

Typical optical losses for both the CO_2 laser receiver and the transmitter are presented in Tables 4-2 and 4-3, respectively. The telescope design configuration for each system is the Gregorian.

Table 4-4 gives weight and loss estimates for three transceivers. Graphs of weight versus primary mirror diameter are shown in Figure 4-5b.

TABLE 4-2. TYPICAL OPTICAL LOSSES FOR CO_2 LASER RECEIVER

Net transmission associated with eight surfaces in the optical train (assumed transmission/ reflection loss at each surface to be 1%)		92.3%
Diplexer transmission of input beam		97%
Diameter obscuration of 20% results in net transmission of detected signal		92.5%
Mixing efficiency at detector		72%
Overall receiver transmission	(0.923)(0.97)(0.925)(0.72) 0.596	
Overall receiver loss	2.25 dB	

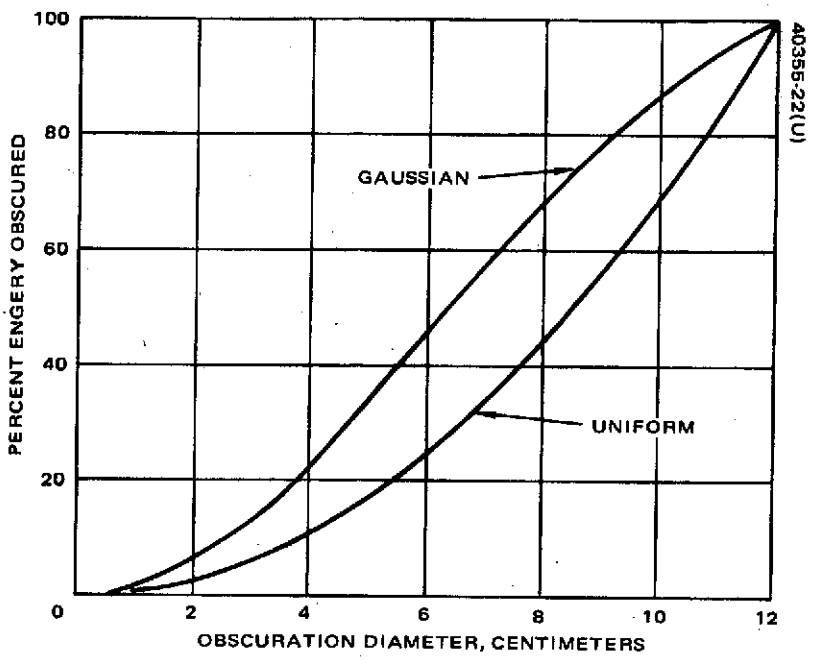

FIGURE 4-7. PERCENT ENERGY OBSCURED FOR UNIFORM AND GAUSSIAN BEAMS USING A 12 CM APERTURE

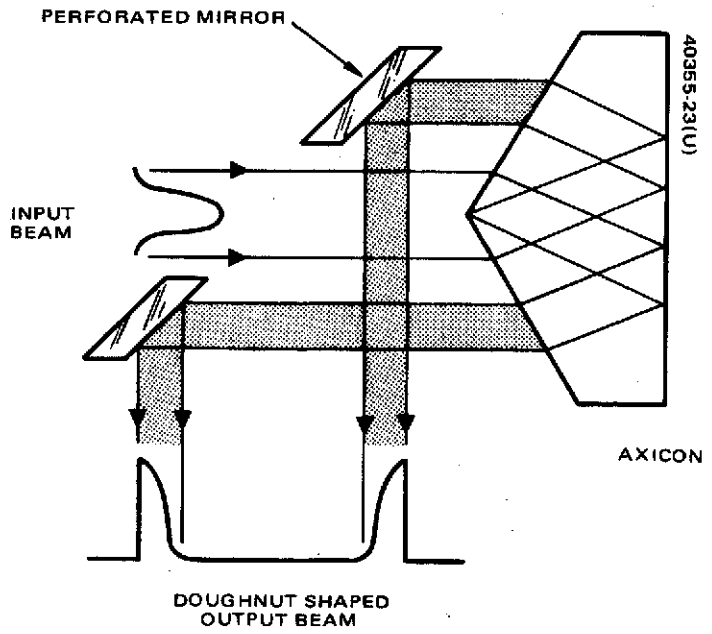

FIGURE 4-8. ENERGY REDISTRIBUTION TECHNIQUE

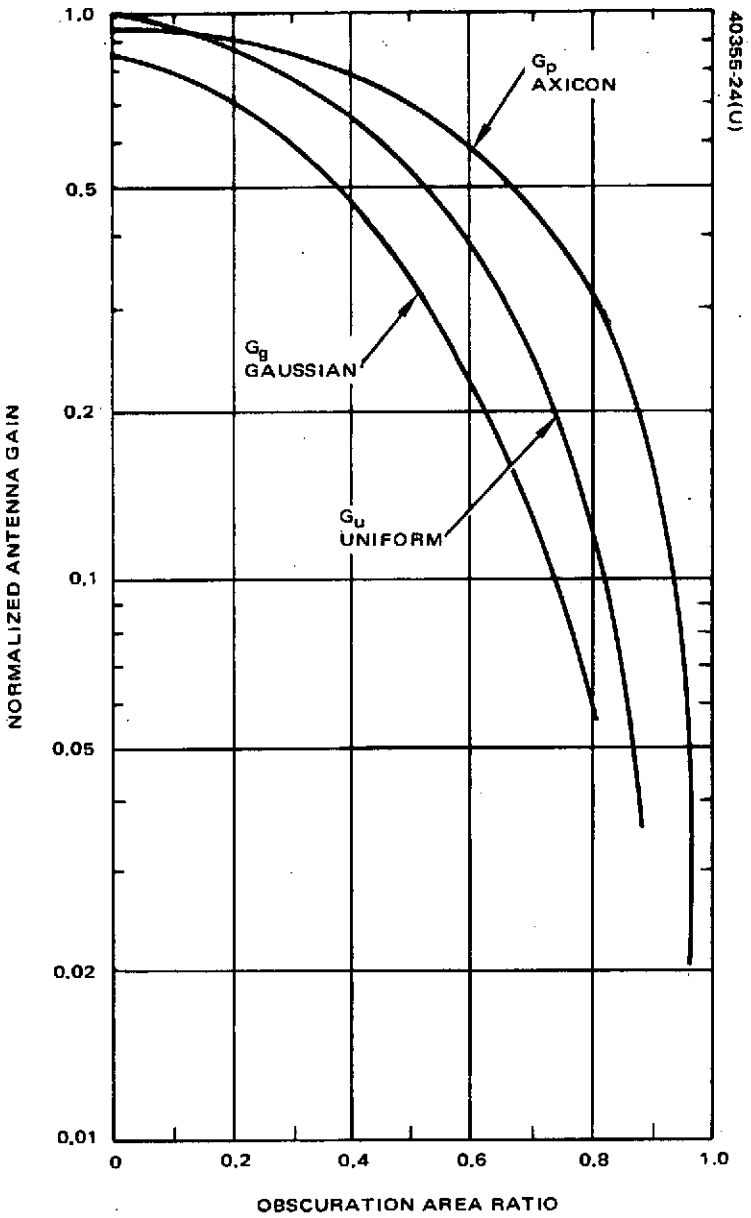

FIGURE 4-9. NORMALIZED ANTENNA GAIN FOR OPTICAL TELESCOPE ILLUMINATED WITH UNIFORM INTENSITY WAVEFRONT (G_u), TEM_{oo} LASER MODE OUTPUT (G_g), AND GAUSSIAN DISTRIBUTION REDISTRIBUTED WITH AXICON (G_p)

TABLE 4-3. TYPICAL OPTICAL LOSSES FOR CO_2 LASER TRANSMITTER

Net transmission associated with four reflecting surfaces in optical train (assumed reflection loss per surface to be 1%)		96.0%
Diplexer transmission of outgoing beam		91.0%
Diameter obscuration of 20% results in net transmission of Gaussian amplitude beam		71%
Transmission of a four lens zoom system for beacon		91.4%
Overall transmitter efficiency	(0.96)(0.91)(0.71)(0.914) 0.567	
Overall transmitter loss	2.46 dB	

TABLE 4-4. CO_2 LASER TRANSCEIVERS WITH WEIGHT AND LOSS ESTIMATES

System	Primary Mirror Diameter, cm	Optics Weight With Mountings, lb	Transmitter Losses, dB	Receiver Losses, dB
Three-Axis	14	4.7	2.46	2.25
Two-Axis	18	6.7	2.46	2.25
Two-Axis	27	16.0	2.46	2.25

4.4 LASER TRANSMITTER PACKAGE WEIGHT AND ELECTRICAL EFFICIENCY

4.4.1 Weight

The package weight for the transmitter laser, modulator, and modulator driver is a function of the transmitter output power. For the particular case of a 300 Mbps system, an expression for the approximate package weight can be stated.

Power Conditioning

The power conditioning weight is approximately 10 pounds for every watt of laser output power. Weight = 10 P where P is the modulated laser output power.

Laser

The minimum weight of the laser is about 5 pounds including the modulator and modulator driver. This weight increases with the laser output power because the laser is larger and the modulator driver is larger. It is approximated by weight = 5 = $(2P)^2$.

Opto-Mechanical Factors

Structure weight also scales with the laser output power in that greater strength must be provided in the structure to support the heavier laser modulator and modulator driver. This additional weight is approximated by weight = 5 + P. The net weight of the transmitter as a function of laser transmitter output power is shown in Figure 4-10 and is represented by

$$\text{Total weight} = 10 + 11\,P + 4\,P^2 \text{ pounds}$$

4.4.2 Electrical Efficiency

Laser transmitter efficiency is determined by a power tradeoff analysis of the laser and modulator driver. Optimum pressures and gains have been determined for any given laser circulating power, and the tradeoff between modulator driver lever and laser circulating power is used to determine the overall optimum power division between the laser and driver. Data for these estimates are preliminary and must be updated as the program progresses. The resulting efficiencies as a function of laser transmitter output power is given in Figure 4-11.

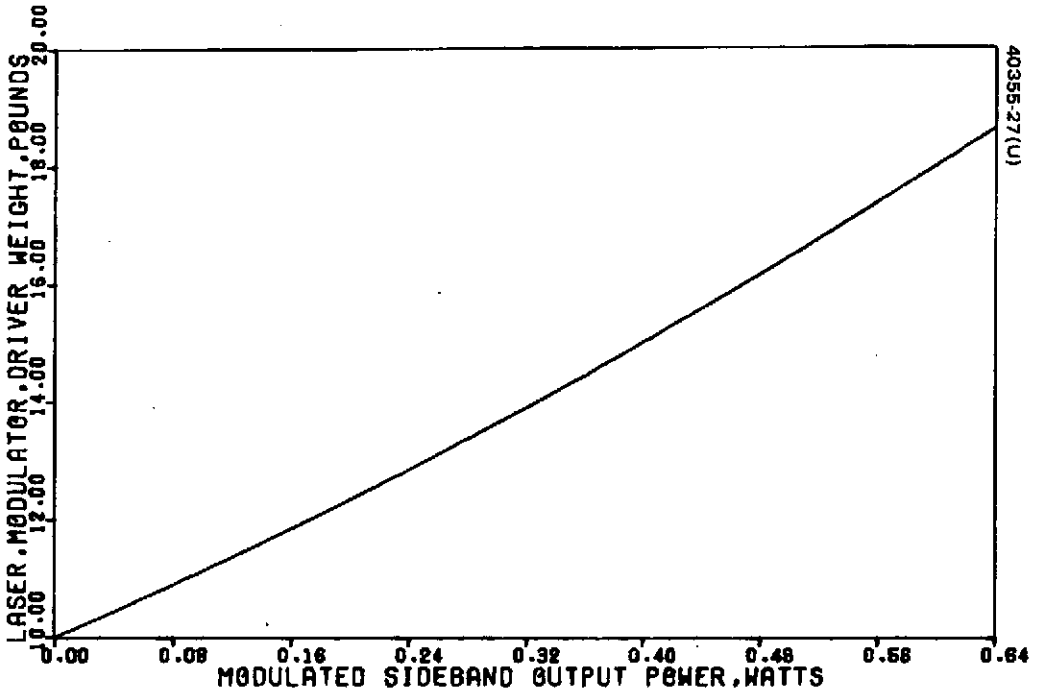

FIGURE 4-10. LASER TRANSMITTER WEIGHT VERSUS OUTPUT POWER

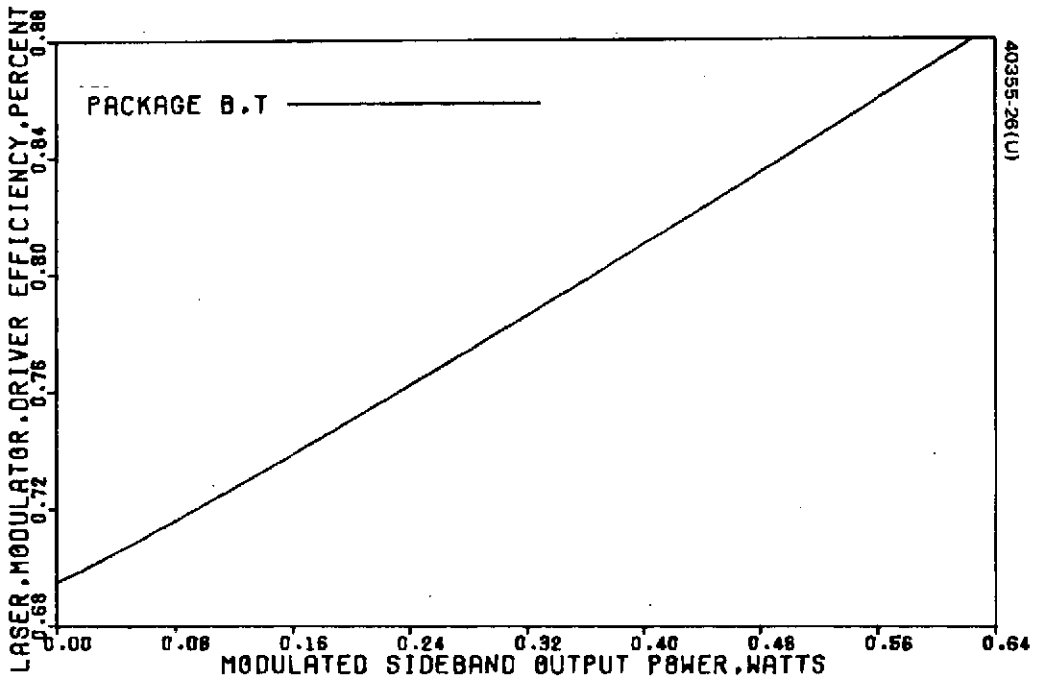

FIGURE 4-11. LASER EFFICIENCY VERSUS OUTPUT POWER

5. LINK OPTIMIZATION AND ANALYSIS

5.1 OBJECTIVES

In principle, the specified Laser Data Relay Link (LDRL) performance requirements can be met by a continuum of similar systems each with an appropriate combination of transmitter and receiver aptertures (D_T and D_R) and transmitted power (P_T). Even within the realm of sensibly realizable combinations, wide variations in these fundamental system parameters are possible. From these possibilities then, one such combination must be chosen which (by some meaningful criterion) results in a "best" system. For spaceborne systems, one meaningful measure of "best" is lightest, all else being equal. The determination of the combination of aperture sizes (hence, transmitted power) which results in the lightest weight LDRL system of specified performance was the objective of the optimization effort described here. The minimum weight LDRL is determined by a computer program which uses a direct search technique to minimize system weight expressed as a function of the parameters to be optimized. The same program then generates a detailed system weight tabulation and a link gain-loss summary table for the optimized system.

5.2 LINK ANALYSIS AND OPTIMIZATION PROGRAM DESCRIPTION

The optimization computer program is written in FORTRAN V for the UNIVAC 1108 and uses a variation of Powell's conjugate direction algorithm to minimize a function which determines weight for a LDRL of specified performance. The program link model performance is specified in terms of information bandwidth and received signal to noise ratio. For any mission environment these system performance parameters are uniquely related to the optimization variables of interest (transmitter and receiver aperture sizes and transmitted power). In the program, the weight of each system constituent is functionally related to transmitter or receiver aperture diameter, transmitter power, information bandwidth, or combinations thereof. The required information (output) bandwidth and signal to noise ratio are specified by the user, and the program judiciously chooses the aperture diameters so that the combined total spaceborne system weight is minimized.

Explicit program inputs which specify link parameters and component characteristics are presented in the following section. Implicit program

inputs are the subsystem weight functional relationships illustrated and discussed in Section 4.

Program outputs are a tabulation of optimum aperture diameters, transmitted power, and weights of all major system constituents for each optimization, as well as a link gain-loss summary table. The optimized outputs may be plotted as a function of intermediate frequency (IF) bandwidth.

5.3 SYSTEM PERFORMANCE AND WEIGHT HANDLING

The LDRL signal to noise ratio (S/N) (hence, bit error probability) and output bandwidth (therefore, data rate) are related to the optimization variables (D_T, D_R, P_T) through the range equation,

$$\left(\frac{S}{N}\right)_o = \frac{\left(\frac{G\eta q}{h\nu_c}\right)^2 R_L P_S P_{LO}}{qB_o G^2 \left[\frac{\eta q}{h\nu_c}\left(P_S + P_B + P_{LO}\right) + I_D\right] R_L + 2k\,TB_o} \qquad (1)$$

where

$\left(\frac{S}{N}\right)_o$ = S/N in B_o

G = detector gain

η = detector quantum efficiency

q = electronic charge

h = Planck's constant

ν_c = optical carrier frequency

R_L = detector load resistance

B_o = output or baseband bandwidth

P_S = received signal power

P_B = received background power

I_D = detector dark current

k = Boltzmann's constant

T = postamplifier noise temperature

P_{LO} = local oscillator power

The received signal power is given by

$$P_S = P_T G_T G_R \eta_A \eta_T \eta_R \eta_P \left(\frac{\lambda}{4\pi R}\right)^2 \quad (2)$$

where

P_T = transmitted power

G_T = G_T (D_T), transmitter aperture gain

G_R = G_R (D_R), receiver aperture gain

η_A = atmospheric loss

η_T = transmitter losses

η_R = receiver losses

η_P = pointing loss

R = range

λ = wavelength

while the background power is

$$P_B = W\theta_R B_1 A_R \eta_R \quad (3)$$

where

W = background spectral radiance

θ_R = receiver field of view (solid angle)

B_1 = optical bandwidth

A_R = receiving aperture area

The component performance parameters and losses which characterize the LDRL optimization program performance model are summarized in Table 5-1. The LDRL weight modeling assumptions for each subsystem are discussed in detail in Section 4 and the resultant functional relationships are illustrated. The weight modeling procedure in most instances consisted of fitting a power law relationship ($y = C_1 + C_2 x^{C_3}$) to actual subsystem

TABLE 5-1. SYSTEM CONSTANTS USED IN LDRL OPTIMIZATION

DETECTOR QUANTUM EFFICIENCY,PERCENT	50.
DETECTOR GAIN	1.00
DETECTOR LOAD RESISTANCE,OHMS	50.
DETECTOR DARK CURRENT,MICROAMPS	.100000
POSTAMPLIFIER NOISE TEMPERATURE,DEGREES K	350.
LOCAL OSCILLATOR POWER,WATTS	.002
LOCAL OSCILLATOR DIPLEXER LOSS,PERCENT	1.
DETECTOR MIXING EFFICIENCY,PERCENT	72.
TRANSMITTER OPTICS EFFICIENCY,PERCENT	96.
TRANSMITTER DIPLEXER LOSS,PERCENT	9.
BEACON ZOOM OPTICS EFFICIENCY,PERCENT	91.
RECEIVER OPTICS EFFICIENCY,PERCENT	91.
RECEIVER DIPLEXER LOSS,PERCENT	3.
RECEIVER DIFFRACTION LOSS,PERCENT	8.
BACKGROUND RADIANCE,WATTS/SQ M*MICRON*STERADIAN	.001
DETECTOR FIELD OF VIEW,MICRORADIANS	84.

preliminary design weights for appropriate independent variable (D_T, D_R, or P_T, etc) values in the range of interest. Other relationships were used where indicated by physical considerations (as in the case of laser weight versus output power). The optimization procedure requires only that the system weight function to be minimized be continuous and well behaved.

The weight associated with the prime power requirements (Figure 5-1) corresponds to the approximate specific weight (lb/watt) of solar power systems in near-earth space with appropriate energy storage, power conditioning, and control to provide a regulated bus. The additional laser power conditioning weight is accounted for in the laser weight model. Other dedicated power conditioning weight is specified explicitly.

5.4 MISSION CONSIDERATIONS AND ASSUMPTIONS

The LDRL optimization has been performed only for the link communication function; acquisition performance is not explicitly considered. A beacon acquisition system is included in the detailed weight breakdown, but its weight is constant and so does not affect the optimization. Only the space-to-space link optimization is presented here. It has been assumed that point-ahead angle control is implemented by beam deflection so that the system is always operating on-axis. For point-ahead angles encountered by the LDRL (≈50 microradians) the additional weight required to do so is much less than that associated with the alternative off-axis operation. The communication range of 46,720 km assumed is approximately the maximum between a 185 km orbit shuttle and a Moliniya terminal. A received S/N of 20 dB was dictated by the specified probability of bit error and margin. Other mission considerations such as line of sight angular rates and doppler frequency shifts are considered implicitly in the design and the corresponding weight dependencies of sensitive system elements.

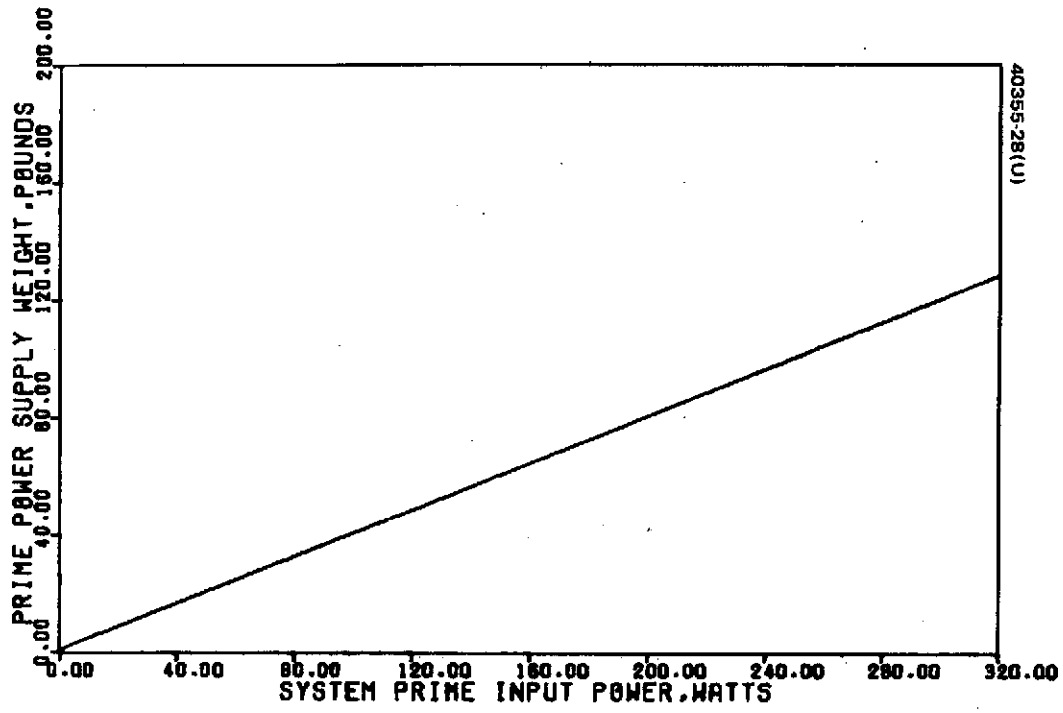

FIGURE 5-1. LDRL PRIME INPUT POWER VERSUS POWER SYSTEM WEIGHT

5.5 RESULTS AND CONCLUSIONS

The LDRL optimization results are indicated in Figures 5-2 through 5-4 and Tables 5-2 and 5-3.

Table 5-2 consists of a detailed weight breakdown for Package A and Package B as optimized for an IF bandwidth of 600 MHz (corresponding to approximately 300 Mbps). The indicated optimized values for Package A and B aperture diameters minimize the total (Package A + Package B) "Associated Weight Burden," which includes the prime power system weight. Certain reliability critical components in the weight tabulations are seen to be followed by a parenthetic redundancy factor permitting the number of such components included for improved reliability to be specified.

Table 5-3 is a tabulation of link gains and losses that expresses the range equation (Equation 1) in logarithmic (decibel) form. The pointing loss entry includes degradation from ideal gain due to nonuniform aperture illumination and secondary obscuration and so is nonzero even though the actual pointing error is assumed to be negligible.

Finally, Figures 5-2 through 5-4 depict optimized parameters of interest for Package A and B as a function of IF bandwidth, for the same link (communication range = 46,720 km, S/N = 20 dB). The interaction of the various weight dependencies of Section 4 may be perceived in the comparison of optimized aperture diameters versus IF bandwidth (Figure 5-2). At smaller aperture diameters, the optimized Package B aperture is smaller than that of Package A because of B's stronger optical weight dependence on aperture. At larger apertures, this disparity is transcended by the stronger Package A structural weight dependence on aperture, and the Package A optimum aperture becomes the smaller. Similar, though less obvious, interactions between all LDRL weight constituents combine to determine the optimum combination of D_T and D_R (hence, P_T) which results in the minimum weight system.

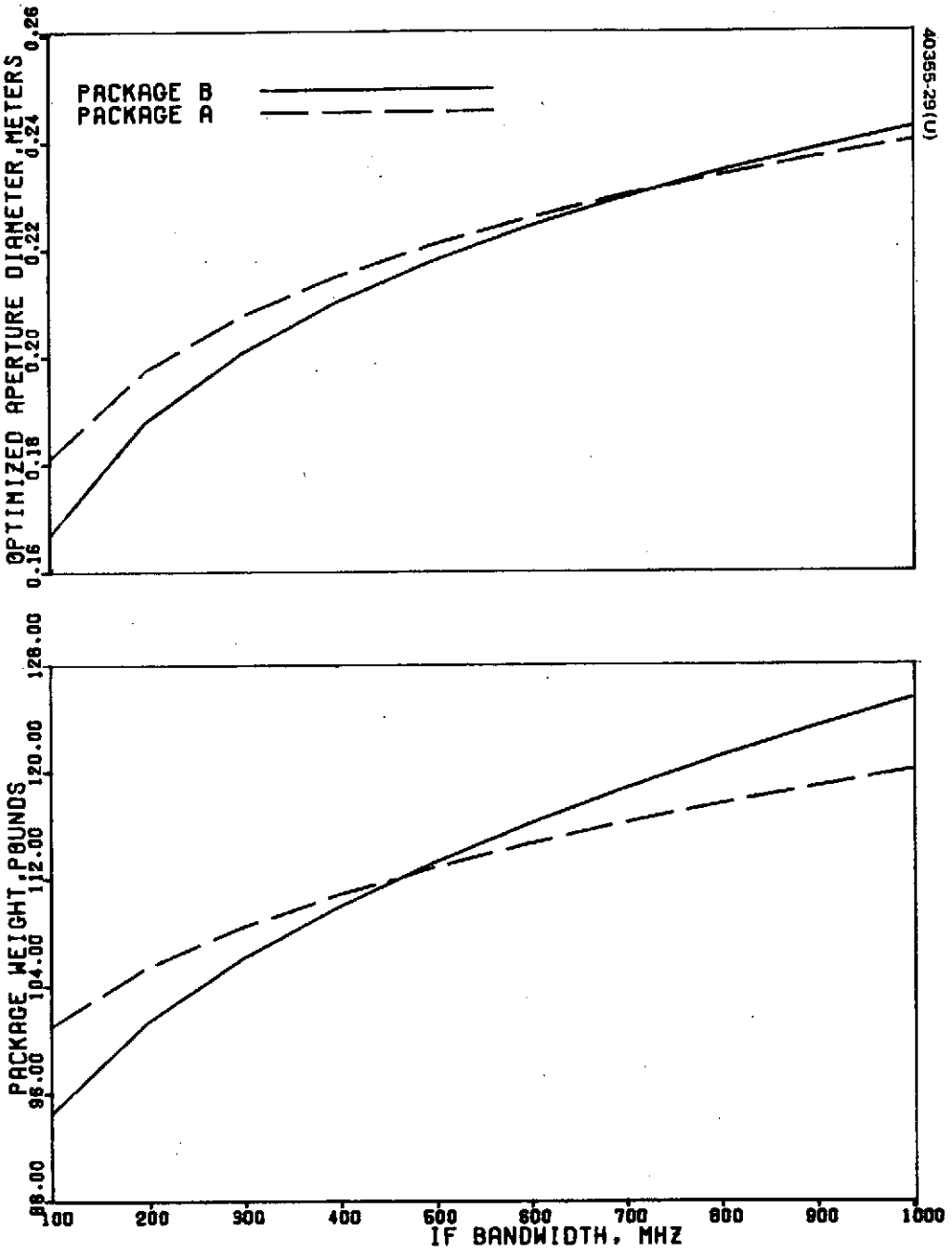

FIGURE 5-2. LDRL PACKAGE A AND B WEIGHT AND OPTIMIZED APERTURE DIAMETER VERSUS IF BANDWIDTH

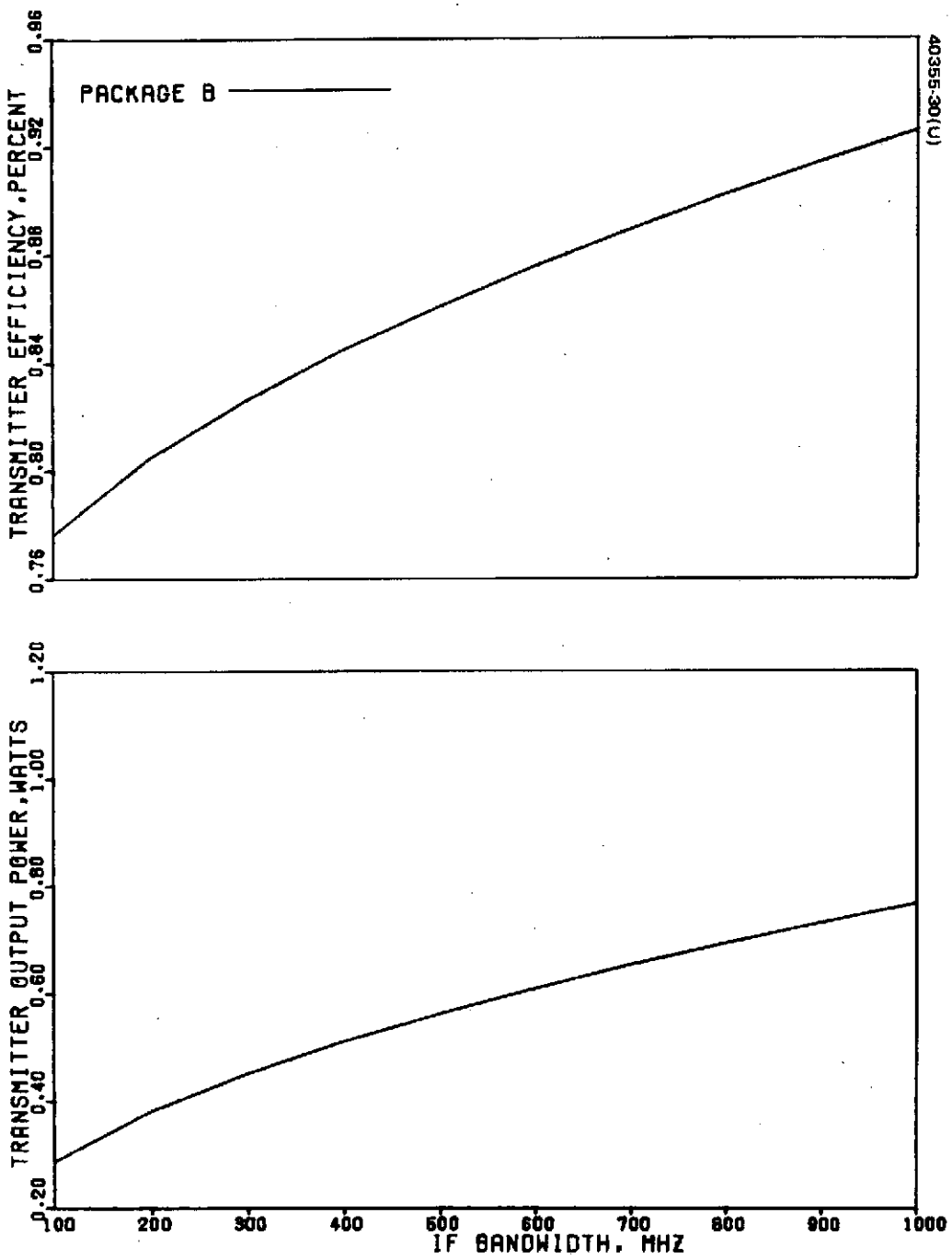

FIGURE 5-3. LDRL OPTIMIZED TRANSMITTER OUTPUT POWER AND TRANSMITTER EFFICIENCY VERSUS IF BANDWIDTH

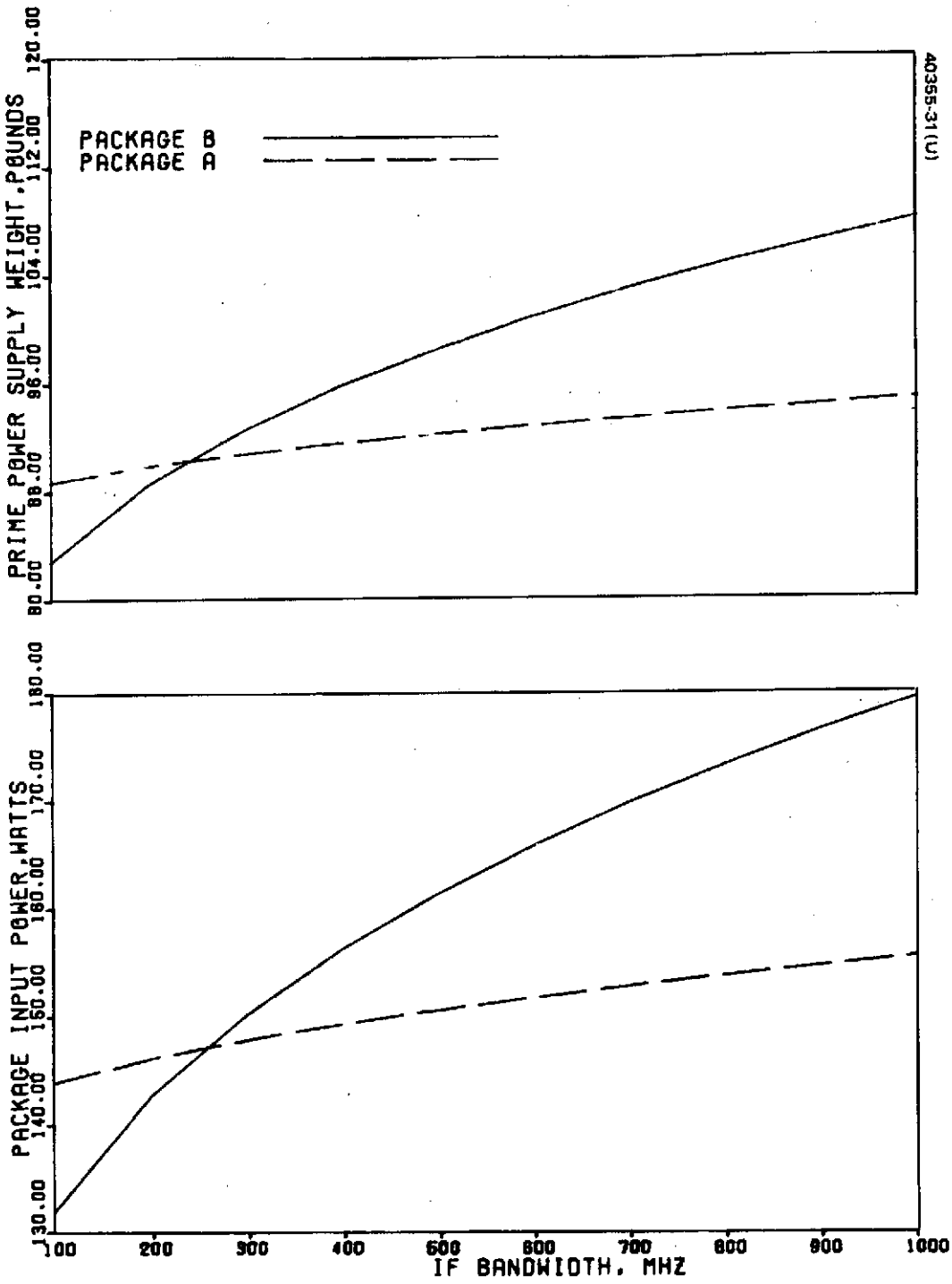

FIGURE 5-4. LDRL PACKAGE A AND B INPUT POWER AND PRIME POWER SUPPLY VERSUS IF BANDWIDTH

TABLE 5-2. OPTIMIZED LDRL WEIGHT AND PARAMETER TABULATION
(RANGE = 46,720 km, S/N = 20 dB)

LINK PARAMETERS VS IF BANDWIDTH

IF BANDWIDTH,MHZ 600.

OPTIMIZED VALUES

PACKAGE B (TRANSMITTER) ANTENNA DIAMETER,M	.2243
PACKAGE A (RECEIVER) ANTENNA DIAMETER,M	.2259
TRANSMITTER OUTPUT POWER,WATTS	.5993
TRANSMITTER EFFICIENCY,PERCENT	.8725

PACKAGE B WEIGHT TABULATION,POUNDS

STRUCTURE WEIGHT	28.70
OPTICAL TELESCOPE WITH MOUNTINGS	12.53
GIMBALS,MOTORS,AND STEERING MIRROR	11.05
SERVO ELECTRONICS	4.77
LASER,MODULATOR,AND MODULATOR DRIVER (1)	18.03
SERVO POWER CONDITIONING	8.03
OTHER POWER CONDITIONING	12.50
DIPLEXER AND MISCELLANEOUS OPTICS	3.06
LASER STABILIZATION ELECTRONICS	.40
BEACON DETECTOR AND POWER SUPPLY (1)	.58
BEACON RECEIVER OPTICS AND ELECTRONICS	.66
IMAGE MOTION COMPENSATION SUBSYSTEM	3.37
CABLES AND CONNECTORS	1.88
MISCELLANEOUS	10.56
PACKAGE B TOTAL WEIGHT	116.11
ASSOCIATED PRIME POWER SYSTEM WEIGHT	100.49
PACKAGE B ASSOCIATED WEIGHT BURDEN	216.61

PACKAGE B POWER TABULATION WATTS

TRANSMITTER LASER INPUT POWER	68.69
TRANSMITTER ELECTRONICS POWER	76.00
POINTING SUBSYSTEM POWER	9.30
BEACON RECEIVER POWER	1.00
CONTROL PANEL POWER	10.00
PACKAGE B SYSTEM POWER	164.99

PACKAGE A WEIGHT TABULATION,POUNDS

STRUCTURE WEIGHT	17.07
OPTICAL TELESCOPE WITH MOUNTINGS	10.48
GIMBALS,MOTORS,AND STEERING MIRROR	11.05
SERVO ELECTRONICS	5.78
RECEIVER AND SIGNAL PROCESSING ELECTRONICS (1)	19.28
SERVO POWER CONDITIONING	7.56
OTHER POWER CONDITIONING	12.00
BEACON LASER (1)	3.00
LOCAL OSCILLATOR LASER (1)	2.00
DETECTOR AND DETECTOR COOLER	4.50
BEAM EXPANDER AND DEFOCUS MECHANISM	.70
IMAGE MOTION COMPENSATION SUBSYSTEM	3.40
CABLES AND CONNECTORS	2.39
MISCELLANEOUS	10.42
PACKAGE A TOTAL WEIGHT	114.63
ASSOCIATED PRIME POWER SYSTEM WEIGHT	92.97
PACKAGE A ASSOCIATED WEIGHT BURDEN	207.60

PACKAGE A POWER TABULATION WATTS

LOCAL OSCILLATOR INPUT POWER	13.00
RECEIVER ELECTRONICS POWER	19.81
POINTING SUBSYSTEM POWER	9.01
BEACON TRANSMITTER POWER	100.00
CONTROL PANEL POWER	10.00
PACKAGE A SYSTEM POWER	151.83

TABLE 5-3. OPTIMIZED LDRL SUMMARY (IF BANDWIDTH = 600 MHz, RANGE = 46,720 km, S/N = 20 dB)

OPTICAL SIGNAL/NOISE PARAMETERS,DB	
TRANSMITTER POWER,W	-2.22
TRANSMITTER OPTICS EFFICIENCY	-.18
TRANSMITTER APERTURE GAIN	96.45
TRANSMITTER DIPLEXER LOSS	-.41
POINTING LOSSES	-1.49
ATMOSPHERIC LOSSES	.00
PROPAGATION LOSS	-274.87
BEACON ZOOM OPTICS LOSS	-.39
RECEIVER APERTURE GAIN	96.52
RECEIVER DIFFRACTION LOSS	-.34
RECEIVER OPTICS EFFICIENCY	-.39
RECEIVER LOCAL OSCILLATOR DIPLEXER LOSS	-.04
DETECTOR MIXING LOSS	-1.43
RECEIVER DIPLEXER LOSS	-.13
DETECTOR DEGRADATION	-.57
PLANCK'S CONSTANT	331.78
CARRIER FREQUENCY,HZ	-134.52
DETECTOR QUANTUM EFFICIENCY	-3.01
NOISE BANDWIDTH,HZ.	-84.77
SIGNAL TO NOISE RATIO	20.00